MOTION OF A MICROSWIMMER IN POISEUILLE FLOW

Andreas Zöttl*[a)] & Holger Stark*
**Institut für Theoretische Physik, Technische Universität Berlin, Hardenbergstraße 36, 10623 Berlin, Germany*

Summary We study the dynamics of a spherical microswimmer in Poiseuille flow. In 2D the motion can be mapped onto the dynamics of an undamped mathematical pendulum. In analogy to oscillating and cirling solutions we identify swinging and tumbling states for the microswimmer in Poiseuille flow. Depending on the value of the Hamiltonian and the flow strength, we classify the swimming states, in particular, the condition for up- and downstream swimming. In narrow channels hydrodynamic interactions between the microswimmer and the channel wall introduce *friction* into the system. This results in stable upstream-oriented swimming in the center of the channel for *pullers* and a specific stable upstream-oriented swinging motion for a *pusher*.

The hydrodynamics of swimming microorganisms in a viscous fluid has become of great interest for physicists [1]. Far away from the microswimmer, the created hydrodynamic flow field in an unbounded, quiescent fluid is often a force dipole p [2]. In their biological environment mircoorganisms often have to respond to fluid flow and confining boundaries leading to interesting phenomena. In bounded Poiseuille flow, for example, swimming *E. coli* bacteria show a net-upstream flux at the walls due to combined effects of flow vorticities and confinement [3, 4].

In our work we study in detail the dynamics of a microswimmer in Poiseuille flow. We assume a spherical swimmer with an intrinsic swimming speed v_0 moving in a cylindrical microchannel of radius R where a Poiseuille flow $\mathbf{v}_f = v_f(1-\rho^2/R^2)\hat{\mathbf{z}}$ is imposed. Therefore we analyze analytically the equations of motion for a microswimmer in flow and numerically the swimmer dynamics by means of multi-particle collision dynamics.

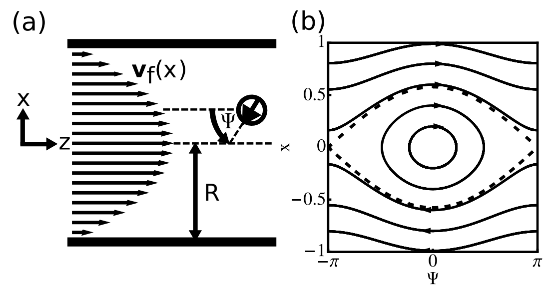

Figure 1. (a) Poiseuille flow $\mathbf{v}_f(x)$ and swimmer coordinates (x, z, Ψ). (b) Ψ-x phase space for $\bar{v}_f = 12$. The separatrix (dashed line) at $H = 2$ devides swinging and tumbling trajectories.

To capture the main ideas, we first focus on trajectories in two dimensions where we describe the state of the swimmer with the distance x from the centerline, the position z in the channel and the orientation angle Ψ (Fig. 1(a)). Due to the translational symmetry in z-direction only the equations for x and Ψ are coupled which leads (after rescaling) to a mathematical pendulum equation ($\ddot{\Psi} = \bar{v}_f \sin\Psi$) [5] where $\bar{v}_f = v_f/v_0$ and x plays the role of a velocity (Fig. 1(b)). The corresponding Hamiltonian is $H = \bar{v}_f x^2/2 + 1 - \cos\Psi$. In analogy to the oscillating and circling solutions of an undamped pendulum, the microswimmer performs either a swinging motion about the centerline oriented upstream on average or a tumbling motion. In contrast to the phase space of a pendulum the formal velocity x is restricted to $x \in \{-1, 1\}$. So, when $H > \bar{v}_f/2$, the swimmer touches the wall. Considering only steric interactions of the microswimmer with the wall, the swimmer reorients at the wall towards the upstream orientation and leaves it at $\Psi = 0$ while the Hamiltonian decreases to $H = \bar{v}_f/2$. Now, we classify the dynamics of the microswimmer in terms of the flow strength $\bar{v}_f$ and the value H of the Hamiltonian. Fig. 2(a) shows the "phase diagram" . We identify regions of swinging motion with a net upstream (A-C) or downstream (D-F) drift and of tumbling motion (G-I). The black area is not allowed since $H < 2 + \bar{v}_f/2$. Fig. 2(b) shows the corresponding trajectories $z(x)$. To determine whether the swimmer moves upstream ($\dot{z} < 0$) or downstream ($\dot{z} > 0$), we use $\dot{z} = \bar{v}_f(1-x^2) - \cos\Psi$ [5]. In region A the swimmer moves upstream all the time, even in the center of the channel where the flow is strongest, so $\dot{z}(x=0) < 0$ leading to $0 < \bar{v}_f < 1 - H$. This changes for region B, where $\dot{z}(x=0) > 0$. Nevertheless, a net upstream motion occurs for $z(x = x_{\text{max}}) < z(x = 0)$ with $x_{\text{max}} = \sqrt{2H/\bar{v}_f}$, so $1 - H < \bar{v}_f \lesssim 1 + H/2$. In region C the swimmer touches the wall, reorients and leaves the wall at $\Psi = 0$ swimming upstream with the maximum amplitude $|x| = 1$. Interestingly, the microswimmer always moves upstream when the flow is sufficiently weak ($\bar{v}_f \lesssim 1$), at latest after contact with the walls. In region D the swimmer moves downstream, $z(x = x_{\text{max}}) > z(x = 0)$, but with upstream segments near the walls, so $\dot{z}(x = x_{\text{max}}) < 0$ and $1 + H/2 \lesssim \bar{v}_f < 1 + 2H$ with $H < 2$. When $\dot{z}(x = x_{\text{max}}) > 0$ (region E) the swimmer moves downstream all the time which is fulfilled for $\bar{v}_f > 1 + 2H$ with $H < 2$. In region F the swimmer effectively drifts downstream with maximum amplitude $|x| = 1$ after contact with the wall. For the tumbling states (G-I) the same conditions apply as for D-F but with $H > 2$.

For swimming in three dimensions the state of the swimmer is given by three cylindrical position (ρ, φ, z) and two orientation (Ψ, Θ) variables. Due to the symmetry in z- and φ-direction, the relevant phase space is three-dimensional (Ψ-x-Θ). We identify two constants of motion leading again to closed orbits around stable fixed points and to open orbits. Swimming at a fixed point now corresponds to a helical trajectory. Closed and open orbits in the (Ψ-x-Θ) phase space are helical-like swinging and tumbling trajectories, respectively.

Now we consider hydrodynamic interactions of the microswimmer with the channel wall. Ref. [6] showed that hydrody-

a) Corresponding author. E-mail: andreas.zoettl@tu-berlin.de.

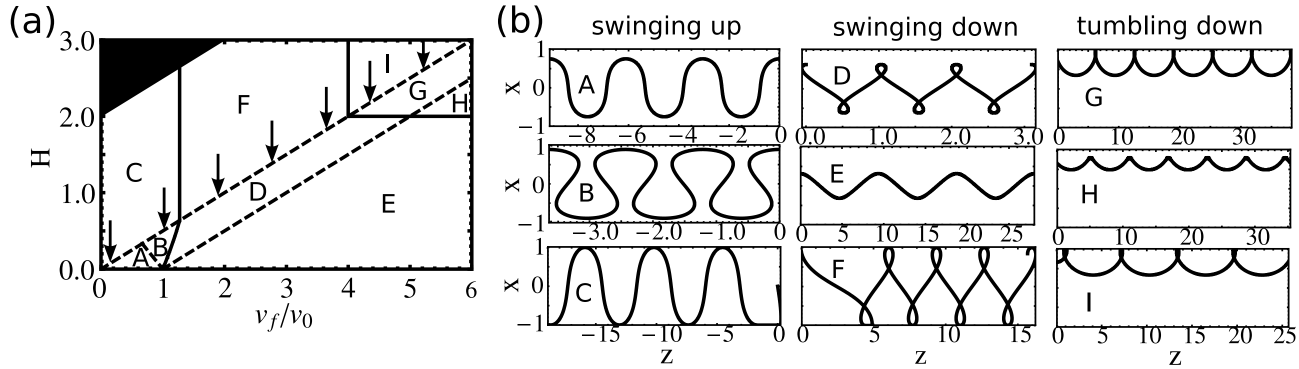

Figure 2. (a) Classification of trajectories $z(x)$ depending on the Hamiltonian H and the flow strength $\bar{v}_f$. *A-C*: swinging state with net upstream motion; *D-F*: swinging state with net downstream motion; *G-I*: tumbling state. *black*: vorbidden area since $H < 2 + \bar{v}_f/2$. Starting in regions C, F, I the microswimmer touches the wall and the Hamiltonian decreases to $H = \bar{v}_f/2$ where the swimmer leaves the wall. This is indicated with black arrows. (b) Examples of all different types of trajectories from regions A to I. All trajectories start at $z = 0$. A: Upstream swinging motion for $\bar{v}_f = 0.7$, $H = 0.2$; B: Upstream swinging motion with downstream segments for $\bar{v}_f = 1$, $H = 0.4$; C: Upstream swinging motion at maximum amplitude after contact with the wall for $\bar{v}_f = 0.5$, $H = 1$; D: Downstream swinging motion with upstream segments for $\bar{v}_f = 1.3$, $H = 0.5$; E: Downstream swinging motion for $\bar{v}_f = 4$, $H = 0.4$; F: Downstream swinging motion with upstream segments at maximum amplitude after contact with the wall for $\bar{v}_f = 2$, $H = 1.8$; G: Tumbling motion with upstream segments for $\bar{v}_f = 5$, $H = 2.3$; H: Tumbling motion for $\bar{v}_f = 10$, $H = 2.2$; I: Tumbling motion with upstream segments after contact with the wall for $\bar{v}_f = 4.5$, $H = 3$;

namic interactions lead to trapping of microswimmers close to a wall. When swimming in narrow channels, the swimmer experiences hydrodynamic interactions all the time. We add wall-induced translational and angular velocities to the equations of motion and assume that in leading order the flow field created by the microswimmer is a force dipole with strength p. Fig. 3 shows phase space plots for for a *puller* ($p < 0$) and a *pusher* ($p > 0$) for $\bar{v}_f = 12$. Repelled by the walls, the swinging motion of a puller is damped and an attractive fixed point exists. A puller tumbling near the wall is attracted by the wall and stays near to it. A pusher, on the other hand, is attracted by the channel walls when oriented upstream but is pushed away from the wall when tumbling near the wall leading to a stable limit cyle in the Ψ-x phase space. To determine the time scale τ, in which a microswimmer approaches its stable trajectory, we linearize the equations of motion around the fixed point ($\Psi = 0, x = 0$) and obtain $\tau = -64\pi\eta R^3/(3p)$ [5], where η is the viscosity of the fluid. For example an *E. coli* bacterium with $p \approx 0.8pN\mu m$ [7] in water should reach a stable swinging trajectory within seconds.

To conclude, mapping the motion of a microswimmer onto the classical pendulum equation, allowed us to identify swinging an tumbling trajectories for a spherical microswimmer in Poiseuille flow. We first classified the swimming states for 2D trajectories and showed that at low and medium ($v_f \approx v_0$) flow strengths a swimmer effectively moves upstream. Hydrodynamic interactions between the swimmer and walls lead to dissipative dynamics in phase space. Pullers are stabilized oriented upstream in the center of the channel whereas pushers perform stable oscillations around the centerline with a specific amplitude.

References

[1] Purcell E. M.: Life at low Reynolds number. *Am. J. Phys.* **45**, 3, 1977.
[2] Lauga E., Powers T. R.: The hydrodynamics of swimming microorganisms. *Rep. Prog. Phys.* **72**, 096601, 2009.
[3] Hill J., Kalkanci O., McMurry J. L., Koser H.: Hydrodynamic Surface Interactions Enable *Escherichia Coli* to Seek Efficient Routes to Swim Upstream. *Phys. Rev. Lett.* **98**, 068101, 2007.
[4] Nash R. W., Adhikari R., Tailleur J., and Cates M. E.: Run-and-Tumble Particles with Hydrodynamics: Sedimentation, Trapping, and Upstream Swimming. *Phys. Rev. Lett.* **104**, 258101, 2010.
[5] Zöttl A., Stark H.: Nonlinear dynamics of a microswimmer in Poiseuille flow. *submitted to Phys. Rev. Lett.*, 2012.
[6] Berke A. P., Turner L., Berg H. C., Lauga E.: Hydrodynamic Attraction of Swimming Microorganisms by Surfaces. *Phys. Rev. Lett.* **101**, 038102, 2008.
[7] Drescher K., Dunkel J., Cisneros L. H., Ganguly S., Goldstein R. E.: Fluid dynamics and noise in bacterial cell-cell and cell-surface scattering. *Proc. Natl. Acad. Sci. USA* **108**, 10940 (2011).

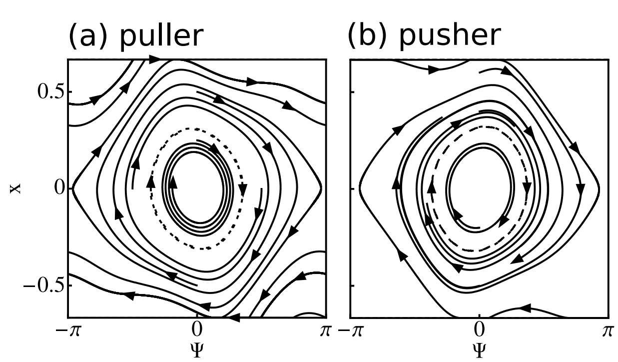

Figure 3. Ψ-x phase spaces for a puller (a) and a pusher (b) at $\bar{v}_f = 12$. The dashed limit cycles are unstable for a puller and stable for a pusher whereas the fixed point at $(0, 0)$ is stable for a puller and unstable for a pusher.